Green Chemistry

PAPER

View Article Online
View Journal | View Issue

Cite this: *Green Chem.*, 2022, **24**, 7082

A mild and efficient oxidative degradation system of epoxy thermosets: full recovery and degradation mechanism†

Yuwei Long, Fei Tian, Lan Bai, Wenli An, Xu Zhao, Rongcheng Du, Xuehui Liu, Xuelian Zhou, Shimei Xu * and Yu-Zhong Wang*

Received 5th May 2022,
Accepted 27th June 2022

DOI: 10.1039/d2gc01678h

rsc.li/greenchem

Despite its high energy efficiency, the oxidative degradation of thermosetting resins has some limitations in practical application due to the complexity and non-selectivity of the oxidation reaction. Here, ammonium ceric nitrate (CAN) aqueous solution was used as the oxidative system to achieve complete and controllable degradation of amine cured epoxy resin (EP) and a 99% degradation rate could be achieved in 1 h at 60 °C. Exploration of the mechanism revealed that the hydroxyethyl ether unit had an important role in the degradation, and degradation products with a high molecular weight (M_w > 8000) were obtained. The resin and CAN can be recycled and reutilised as adhesives, and a high-efficiency catalyst, respectively. In particular, commercial carbon fibre reinforced epoxy resin composite (CFRP) can also be recycled by this degradation system, with the acquisition of nearly non-destructive fibres and resin degradation products that can also be used for bonding.

Introduction

Epoxy resin (EP), as the most productive of the thermosets, is widely used for wind turbine blades, in electronic equipment, in aerospace, as floor paint, and in other fields, because of its light weight, high strength, excellent electrical properties, good corrosion resistance, and excellent adhesion.[1,2] The global EP market value is expected to grow from USD 21.5 billion in 2016 to USD 37.3 billion in 2025.[3] The EP-based materials are different from disposable plastics, in that they have a long lifetime of 10–30 years so that their recycling has not aroused enough attention before. The problem is becoming imperative with the massive decommissioning of the materials in recent years.[4–9] The number of relevant articles published in the literature in the past five years is about 10 times greater than the number published from 2006 to 2010, showing a explosive growth when using epoxy resin, degradation, and recycling as keywords to search in the *Web of Science database*. However, it is very challenging for EP to realise high-efficiency recovery and high-value reutilisation due to the insoluble and infusible properties of the thermosetting EP which are ascribed to a densely crosslinked network structure.

There are two different strategies for the recovery of EP. One is to design new recyclable EP resins by introducing dynamic bonds, which are stable during the application period and can be recycled by heating or solvolysis once they are out of service.[10,11] The reversible dynamic bonds have a positive effect on recycling and reuse of the EP thermosets, but the strategy builds the new type of EP thermosets at the sacrifice of performance and cost. In addition, it cannot handle the existing wastes from the EP thermosets that have been produced and those which will be produced in the future. A different method to the others is to recycle the existing EP wastes using physical or chemical methods.[7] Chemical recovery is regarded as a promising and flexible method because it can degrade EP into useful chemicals. Despite some success in the degradation of EP into small molecule chemicals, the vigorous degradation conditions always lead to high energy consumption, (*i.e.*, in supercritical or subcritical solvents at high temperatures of 200–450 °C and high pressures between 5–30 MPa, or in an extremely high concentration of unsaturated coordination salt solution with temperatures over 200 °C).[12,13] In comparison, oxidative degradation has significant advantages in energy efficiency which can be performed at atmospheric pressure with a temperature lower than 90 °C.[14–25] Use of common oxidants or catalysts has been reported for the degradation of EP including hydrogen peroxide,[14,16,25] nitric

Collaborative Innovation Center for Eco-Friendly and Fire-Safety, Polymeric Materials (MoE), State Key Laboratory of Polymer Materials Engineering, National Engineering Laboratory of Eco-Friendly Polymeric Materials (Sichuan), College of Chemistry, Sichuan University, Chengdu 610064, China.
E-mail: xushimei@scu.edu.cn, yzwang@scu.edu.cn

† Electronic supplementary information (ESI) available. See DOI: https://doi.org/10.1039/d2gc01678h

acids,[18,21,22,24] ruthenium trichloride,[15] sodium hypochlorite,[19] potassium permanganate,[20] and so on. Among these, hydrogen peroxide is preferred because of its high redox potential and clean process with water as the only by-product.[14,16,25] Varughese's group successfully performed the oxidative degradation of EP composites using nitric acid/hydrogen peroxide (HNO_3/H_2O_2) or acetic acid/hydrogen peroxide ($HOAc/H_2O_2$) at 65 °C.[14,25] However, the non-selective chemical bond cleavage caused by the high activity hydroxyl radicals leads to the uncontrolled degradation of the resin. The complex degradation products with a low molecular weight of less than 500 were obtained, but they are difficult to separate to use for high value-added reuse. However, ruthenium trichloride can be used for the directional degradation of ER as a catalyst whose reduction product is reoxidised by ammonium ceric nitrate (CAN). However, a special resin structure is required. In addition, it is also very difficult to separate and purify low molecular weight degradation products. Despite the energy efficiency, there are some limitations in the application of the oxidative degradation of thermosetting resins due to the complexity and non-selectivity of the oxidation reaction. There is a lack of research on the in-depth mechanisms, and the "blind box" of oxidative degradation leads to complex small molecule degradation products, as well as low reutilisation of the degradation products.

In our very recent work, we found that the degradation efficiency in the HNO_3 oxidation system was significantly increased (by 30 times) after crushing and introducing some pores, which were induced by swelling, into the EP thermosets.[22] Meanwhile, the degradation products with a higher molecular weight (M_w > 8000) were obtained because the skeleton structure of the EP was retained under the milder reaction condition. Such degradation products were easy to separate, and were endowed with high-value utilisation in the field of oil–water separation or substance purification. Unfortunately, the HNO_3 cannot be recycled well in the system, which leads to low nitrogen utilisation and potential secondary pollution, and the relationship between fine structure and redox active sites remains unclear. These results inspired us to further develop a new oxidation system to give a greener degradation process and it was able to achieve full recovery of the whole degradation system using in-depth mechanism exploration.

Using CAN as an oxidant has the advantages of excellent oxidation efficiency and ease of storage and transport. Herein, CAN is used to replace HNO_3 for the oxidative degradation of amine-cured EP. A high degradation rate of 99% can be obtained in the CAN aqueous solution after reacting for 1 h at 60 °C. Similarly, the degradation products show a high M_w of more than 8000. Nearly complete conversion and recovery of the amine-cured EP were achieved. Even more, after the degradation products were separated by simple filtration, the reaction solution can be concentrated and crystallised to obtain high-purity cerium(III) ammonium nitrate tetrahydrate [$(NH_4)_2Ce(NO_3)_5{\cdot}4H_2O$]. It is generally believed that the oxidative degradation of the amine-cured EP was basically attributed to the cleavage of the C–N bonds. In our present work, it was found that it was the hydroxyethyl ether unit which had an important role in the degradation under the CAN system, and thus a degradation mechanism was proposed. Furthermore, the system also performs well in the recycling of commercial carbon fibre reinforced epoxy resin composite (CFRP).

Experimental section

Materials

The E-51 epoxy resin, and the curing agent, 4,4-diaminodiphenyl methane (DDM), were purchased from the Bluestar Chemical Company, and the Aladdin Chemicals Company, respectively. Commercial CFRP was provided by Sichuan Dongshu New Materials Company. Cerium ammonium nitrate (CAN, ≥98%) was purchased from Adamas Reagent Company. Other solvents were obtained from Chengdu Kelong Chemical Reagent Company (China). All the chemicals were used as received without further purification.

Method

Degradation of EP. The DDM-cured EP was prepared according to a method used in our previous work.[22] Prior to chemical degradation, the EP was pulverised and then allowed to swell in *N*-methyl pyrrolidone (NMP, 1 : 5, w/v), which was assisted by microwave radiation at 120 °C for 2 h. After washing with deionised water followed by drying in the oven, the swollen EP (SEP) were obtained for use in the subsequent degradation. Typically, 1.0 g SEP (m_0) was added to 5 mL of 1.75 mol L^{-1} of CAN aqueous solution, and the degradation was conducted at 60 °C for 1 h in a water bath. Afterwards, the solid was repeatedly washed with distilled water to remove the residual CAN before being dried. To separate the undegraded resin from the solid, the solid was placed in DMSO to dissolve the degradation products of SEP (DSEP). The undissolved parts were dried and weighed (m_1). The degradation ratio (D_r) was calculated according to eqn (1). The filtrate was collected, and the solvent was removed by rotary evaporation and further concentrated for crystallisation. The obtained solid is presented as r-salt and the solvent removed can be recycled.

$$D_r = (m_0 - m_1)/m_0 \times 100\% \quad (1)$$

Characterisation and measurements

The Fourier transform infrared (FTIR) spectra were obtained using a Nicolet 6700 FTIR spectrophotometer over the wavelength range of 4000–400 cm^{-1} with a resolution of 4.0 cm^{-1}. The specimen for the FTIR experiment was prepared by grinding 1 mg of each sample with 50–100 mg of fresh FTIR grade KBr, and then the powder was compressed into a tablet under 20 MPa applied force for 30 s. X-ray photoelectron spectroscopy (XPS) spectra were obtained using a Kratos XSAM800 spectrometer (UK). The glass transition temperature (T_g) was measured using a TA Instruments Q200 differential scanning calorimeter (DSC) at a scan rate of 10 °C min^{-1}, scanned from

40 °C to 200 °C under a nitrogen atmosphere (50 mL min^{-1}). Liquid-state nuclear magnetic resonance (NMR) spectra were obtained using a Bruker Avance III HD (400 MHz) spectrometer. The deuterated dimethyl sulfoxide was used as solvent, and tetramethyl silane was used as the standard. Gel permeation chromatography (GPC), with an Agilent 1100 capillary LC system, was used to evaluate the M_w, with polystyrene as the standard and *N*,*N*-dimethylformamide (DMF) as the mobile phase. The scanning electron microscopy (SEM) images of the samples were taken using a ThermoFisher Scientific Phenom Pro X instrument (The Netherlands). Prior to the SEM imaging, the sample was sputter coated with an Au layer to improve the conductance. The porosity of the SEP was tested using a Micromeritics AutoPore 9500 automatic mercury porosimeter. The elemental analysis (EA) was performed on an Elementar Vario EL cube element analyser (Langenselbold, Germany). The degradation products were added into ethyl acetate and the extract were analysed by gas chromatography-mass spectrometry (GC-MS) on a Shimadzu GCMS-QP2010 UItra. A single lap tensile shear strength test was performed in an Instron 3366 electronic universal material testing machine according to the GB/T 7124-2008/ISO 4587:2003 standards. The load of the sensor was 1 kN, and the tensile speed was 2 mm min^{-1}. The tensile strength of single carbon fibre was determined on an electronic single fibre strength tester (Laizhou Electronic Instrument Company, China) with a tensile speed of 5 mm min^{-1} in accordance with the GB/T 31290-2014 standard.

Results and discussion

Oxidative degradation of epoxy thermosets by CAN

Similarly to our previous work,[22] the introduction of the pores into the EP matrix could significantly improve the mass transfer and in turn facilitated the degradation (see the ESI for details†). In this work, CAN was used as oxidant agent instead of HNO_3 which made the degradation easy to control. When the CAN concentration was 1.75 M, the resin can be completely degraded at 60 °C within 60 min (Fig. 1). In addition, increasing the reaction time and the reaction temperature also positively promoted the degradation of the resin. A high degradation ratio of 99% was achieved at 60 °C for 1 h. Further extension of the time or increasing the temperature will no longer significantly promote the degradation. Instead, the degradation rate even decreased when the temperature was increased above 60 °C due to excessively violent reactions. It was noticed that the product was dark green at a low degradation ratio but turned to brown-yellow at a high degradation ratio (Fig. S2, ESI†). The colour change to dark green may be related to N protonation, and a conjugated structure was formed by further electron transfer.[26]

Degradation mechanism

It was found that the molecular weight of the degradation product was heavily dependent on the oxidant type. In this work, the M_w was as high as 8000 which was close to that for HNO_3.[22] The polydispersity index (PDI) of the degradation product was about 1.9. It can be inferred from this that the degradation product contains 3–5 repeat units (Scheme S1, ESI†). Moreover, the decrease of M_w was not obvious with the extension of the degradation reaction time. It was speculated that with the progress of the degradation reaction, the oxidant was gradually consumed, leading to the decreased oxidisability of the reaction solution. So, the further reaction was difficult to carry out (Table 1, Figs. S3 and S4, ESI†).

However, when H_2O_2 was used, small molecule degradation products with M_w of several hundreds were usually obtained.[25] Moreover, the M_w of the degradation products showed an obvious decrease so that the products experienced a transition from hydrophobic to hydrophilic as the time in the H_2O_2 system was extended. This result confirmed that the degradation was controllable in our system.

For DSEP, the relative absorbance intensity of the C–N peak at 1110 cm^{-1} decreased from 2.8 to 1.2 compared with the original resin, using the absorbance intensity of the C–H

Table 1 The molecular weight and PDI of DSEP at different degradation times

Sample	Reaction time (h)	M_w	M_n	PDI
DSEP-1 h	1.0	8154	3967	2.056
DSEP-2 h	2.0	7279	3958	1.839
DSEP-3 h	3.0	6975	3682	1.922

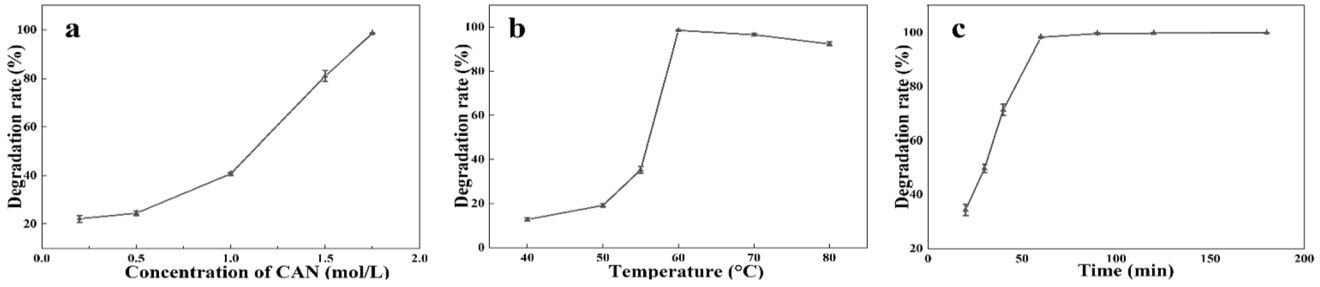

Fig. 1 The effect of the reaction conditions on the degradation rate of SEP: (a) concentration of CAN (60 °C, 1 h); (b) reaction temperature (1.75 M CAN, 1 h); and (c) reaction time (1.75 M CAN, 60 °C).

stretching vibration band at 2966 cm^{-1} as a reference, which confirmed the C–N bond breakage during the degradation process.[27] In addition, the peak of DSEP at 3350–3600 cm^{-1} shifted to a low wavenumber, which was attributed to the formation of an N–H bond after the C–N bond had broken.[28] The presence of the nitro group was supported by two new peaks that arose at 1343 cm^{-1} and 1539 cm^{-1} in the spectrum. This proved that the benzene ring on the resin backbone was nitrated during the degradation process (Fig. 2).[24] It was calculated that A(1539 cm^{-1})/A(2966 cm^{-1}) increased from 0.57 to 1.5 after degradation. For the ^{1}H-NMR spectra of DSEP, it was found that nitrification would cause changes in the chemical shifts of hydrogen at a, b and g but mainly shifts and splits (DGEBA: a,b-7.07–6.84(dd), g-1.58(s); DSEP-1 h: a′,b′-7.08(br), 6.83(br), 7.2–8.5(m), g′-1.57(m)). These prove that the benzene rings and bisphenol A skeletons were not broken into small fragmented molecules, which means that the main chain structure of the EP was well preserved. The new peak at 8.01 ppm was attributed to the nitrated benzene ring, which was consistent with the FTIR results (Fig. 3). The new peaks between 9 and 10 should be attributed to the aldehyde hydrogen, which may be formed after the destruction of the C–N bonds. The signal of NMP was also found. Maleic acid was used as the internal standard, and the amount of NMP was calculated from the NMR, which accounted for about 2.7% of the DSEP. This resulted in an increase in the N content of approximately 0.387% in DSEP. An obvious increase of N content from 3.09% in EP to 8.77% in DSEP was observed, which was mainly attributed to the nitrification that happened during the degradation. It is worth mentioning that there was also an increase in the N content in SEP (Table S1, ESI†). This was

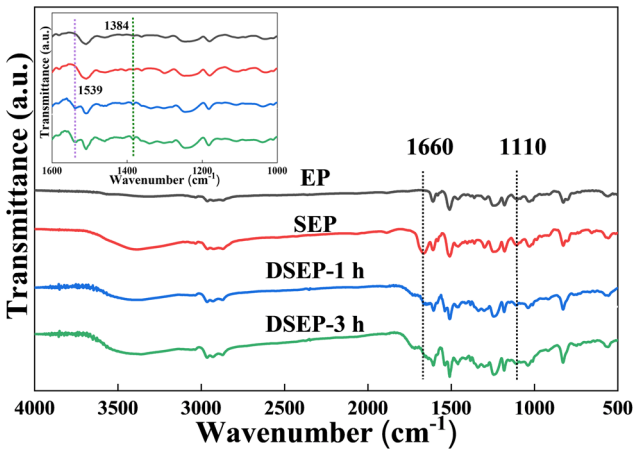

Fig. 2 The FTIR spectra of EP, SEP, and DSEP at different degradation times (inset: the FTIR results of wavelengths from 1000 to 1600 cm^{-1}).

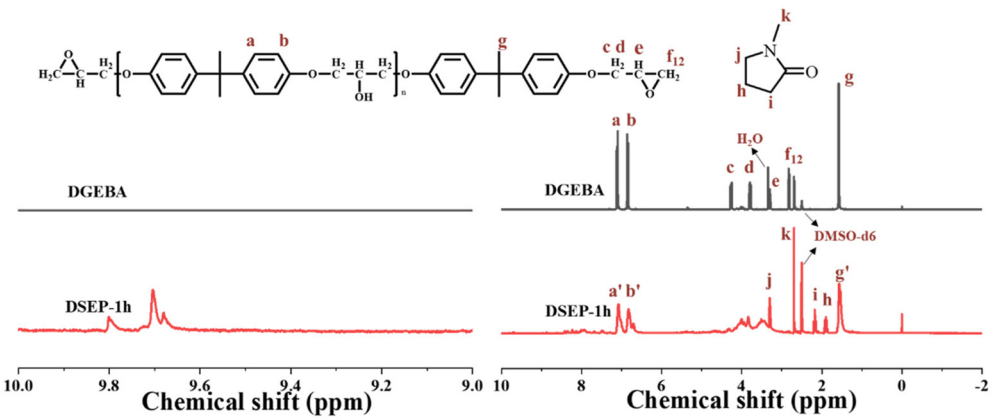

Fig. 3 The ^{1}H-NMR of DGEBA and DSEP.

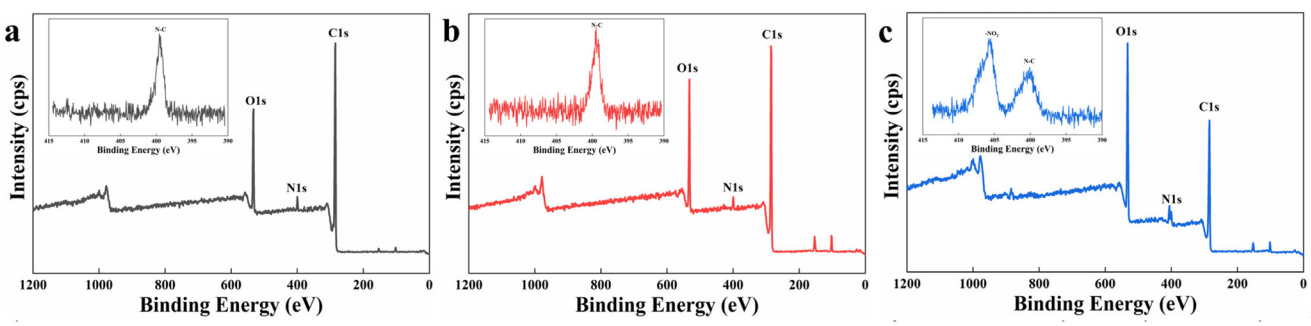

Fig. 4 The XPS and high-resolution N 1s spectra (inset) of (a) EP, (b) SEP, and (c) DSEP-1 h.

caused by the residual NMP due to its strong interaction with EP. Nitrification was further confirmed from the XPS results. There were only three main peaks corresponding to the C element (285.1 eV), O element (533.1 eV), and N element (400.1 eV) in the full spectrum of EP. After the NMP swelling treatment, the atomic orbitals of C, N, and O remained unchanged. Swelling is a physical change that did not destroy the chemical crosslinking structure of the resin, but only increased the chain mobility of the resin. After the resin was degraded by CAN, the N split into double peaks was attributed to the introduction of nitro groups (Fig. 4).

From the previous results, it was inferred that the skeleton structure of the EP was not completely broken during the degradation process. The weaker bonds in the three-dimensional EP system were broken and finally the oligomers formed.

The degradation mechanism could be inferred by clarifying the structure of the degradation product. However, it was only concluded that the cleavage of the C–N in the crosslinks produced N–H and aldehyde groups in the degradation products whereas nitrification happened to introduce nitro group into the benzene ring. It remained unclear how the M_w could be controlled in the CAN system because the M_w decreased to a limited degree (Scheme 1). Unexpectedly, it was observed that the M_w of the degradation products (M_w = 6975) was significantly higher than the ones (M_w = 2833) without NMP treatment. In addition, the existence of NMP was confirmed by both the NMR (Fig. 3) and the GC-MS (Fig. S5 and Table S2, ESI†) results. it was speculated that the strong interaction

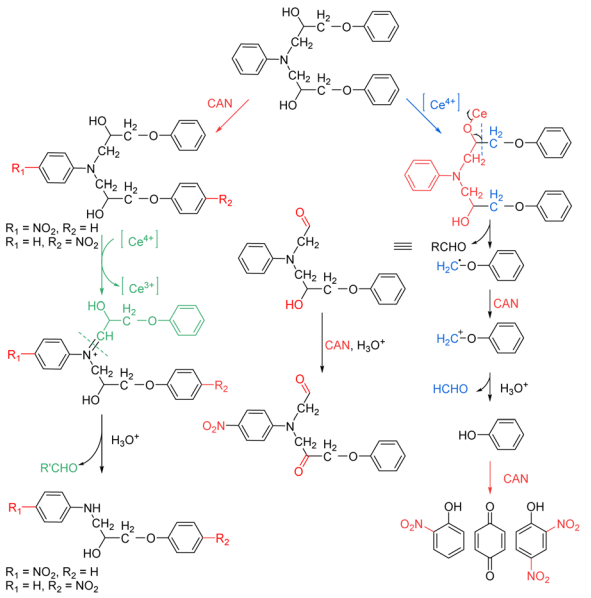

Scheme 2 Proposed mechanism of the model compounds decomposition under the action of CAN.

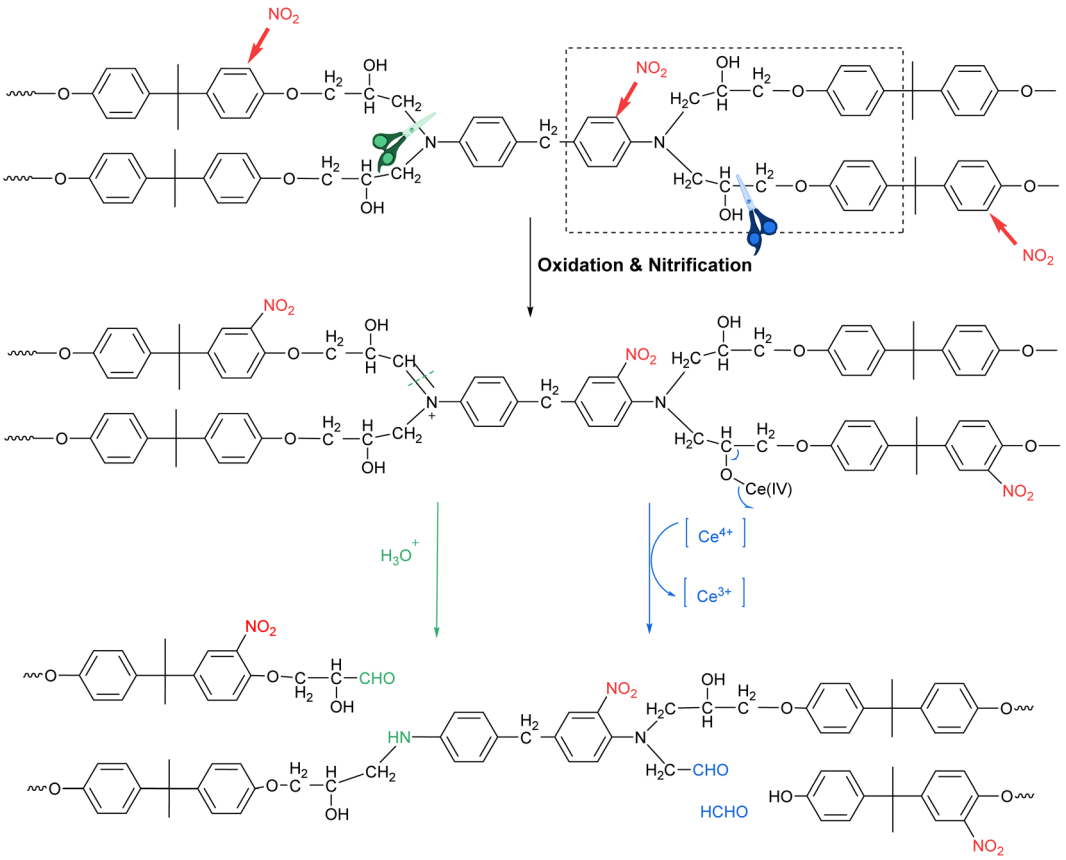

Scheme 1 The proposed mechanism of EP decomposition under the action of CAN.

between the EP and NMP might hinder further degradation. For further mechanism studies, very few of soluble small molecule pieces were extracted by ethyl acetate from the DSEP and analysed by GC-MS (Fig. S5 and Table S2, ESI†). The pieces included bisphenol A, aldehyde, and phenol derivatives, which suggested that cleavage of the C–C and C–O bonds in the hydroxyethyl ether unit had occurred. The possible reaction mechanism was delineated by use of a backward reasoning method.[29–34]

Under the degradation conditions, the hydroxyl groups of the resin participated in the formation of O–Ce(IV) upon the action of cerium(IV), and then the C–C bonds broke into the corresponding aldehydes and carbon radical intermediates by a single electron transfer process (Scheme S2, ESI†).

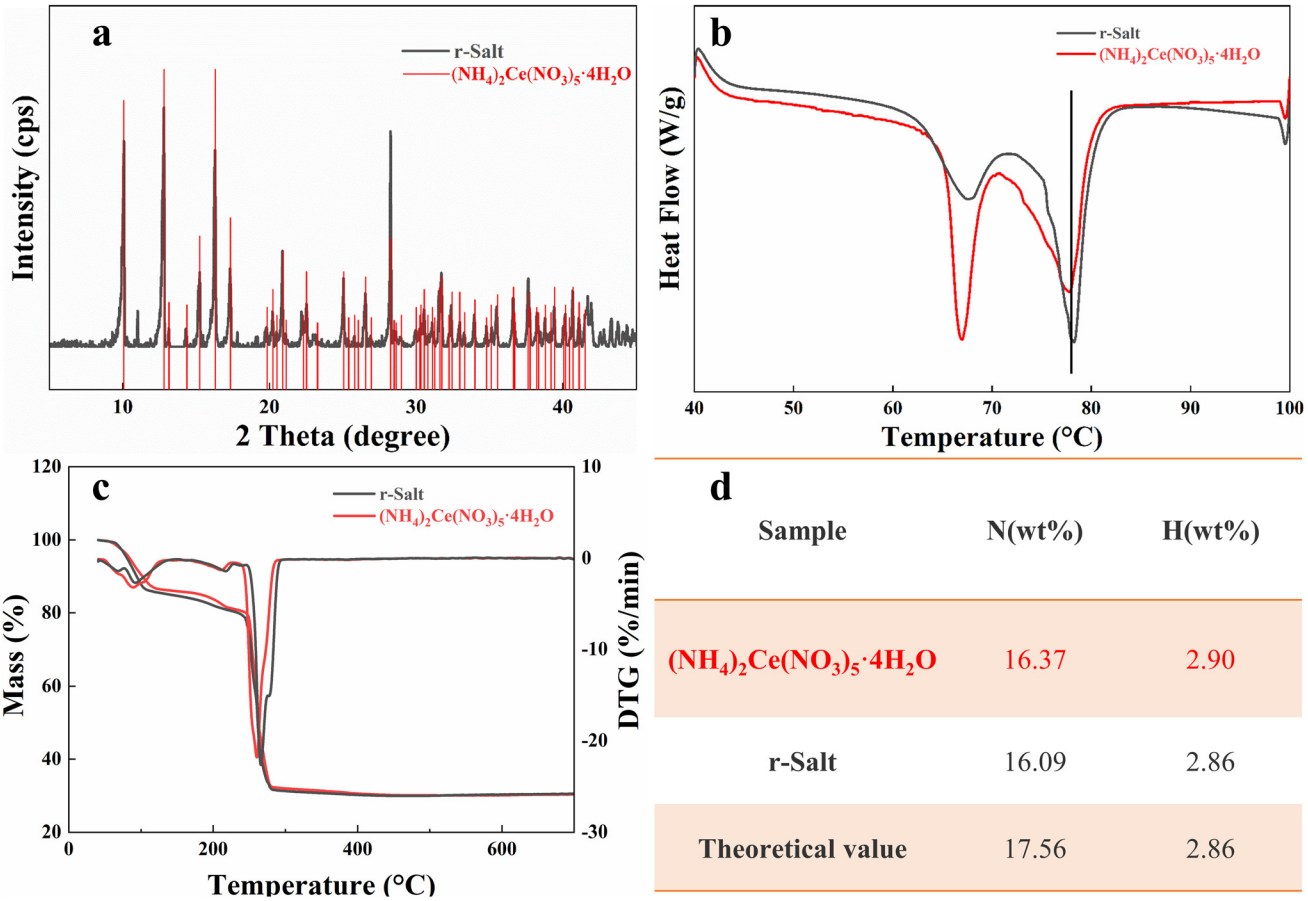

Fig. 5 A series of characterisation tests for (a) XRD, (b) DSC, (c) TGA, and (d) the N and H contents of r-salt and II, and the theoretical value of $(NH_4)_2Ce(NO_3)_5{\cdot}4H_2O$.

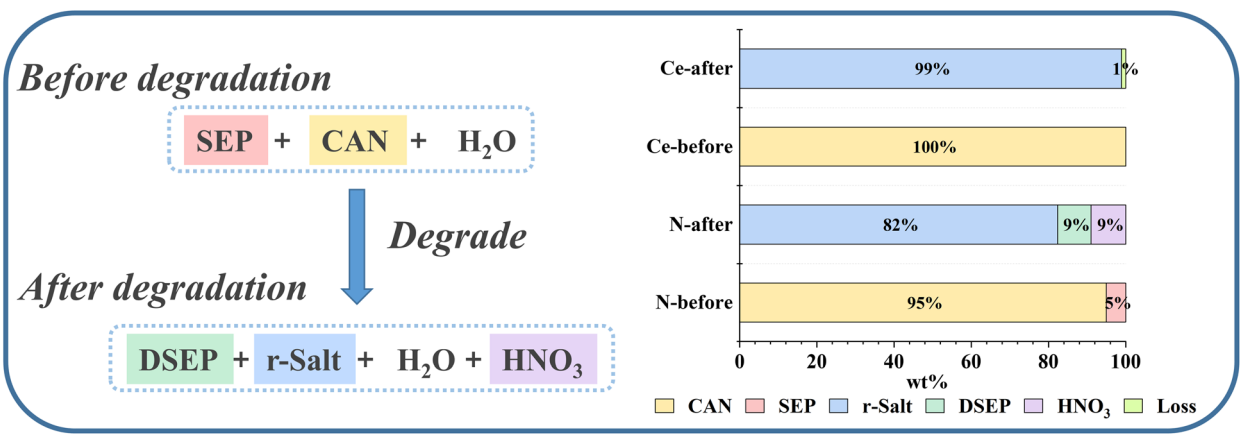

Fig. 6 Direction of flow of Ce and N before and after degradation.

The carbon radical intermediates were further oxidised by cerium(IV) to carbocations, which were attacked by water to form hemiacetals. The hemiacetals were hydrolysed to break the C–O bonds and generate bisphenol A. Under the action of CAN, the bisphenol A underwent a single electron transfer process, C–C bond breaking and nitration simultaneously, resulting in the final small molecule. In the presence of CAN, the EP was nitrated and the amino group was oxidised to an imine cation. Then, the imine was hydrolysed and the C–N bond was broken to form aniline. The amino group was further oxidised to a nitro group to form the final small molecular products. To confirm the mechanism described previously, a model compound was first prepared by the reaction of aniline with phenyl glycidyl ether[35,36] (Scheme S3, ESI†) and then the compound was degraded under the previous conditions, and the degradation products were also analysed by NMR, GC-MS (Fig. S6, S7 and Table S3, ESI†). Except for the residual solvents (acetonitrile, ethyl acetate), the new peaks at 9.70 ppm and 9.73 ppm were attributed to aldehyde hydrogen, which may be formed after the destruction of C–N bonds as well. The fragments detected in the GC-MS test results confirmed the rationality of the degradation mechanism (Scheme 2). This concludes that it is the hydroxyethyl ether structure in the amine cured epoxy resins which act as a key

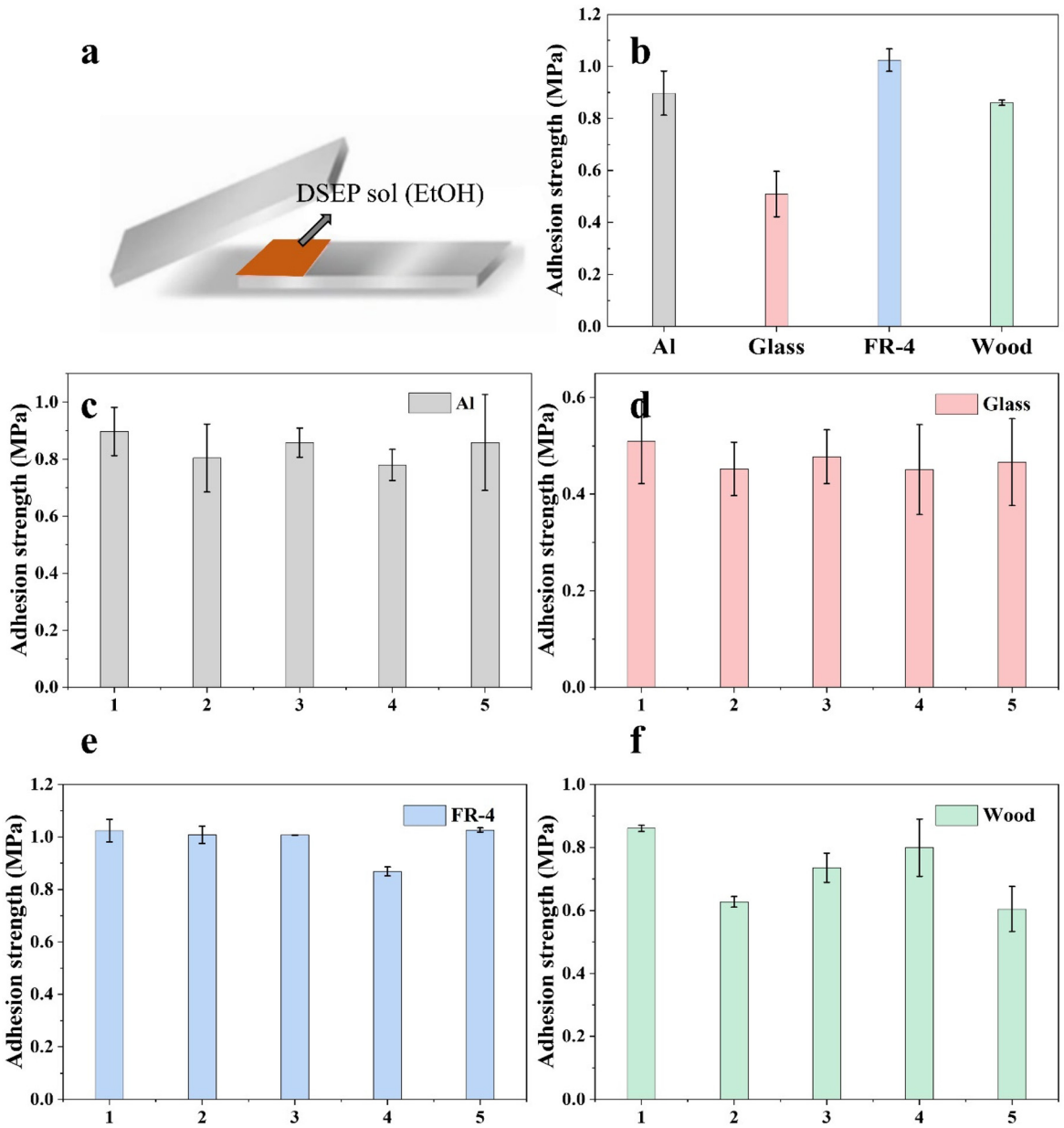

Fig. 7 Use of DSEP for bonding: (a) schematic diagram of the bonding experiment, (b) adhesion strengths for use with different substrates, and (c–f) repeated adhesion to different substrates.

role in degradation. It was further confirmed that the anhydride cured epoxy resins would not be degraded in the same CAN system due to the lack of hydroxyl groups.

Full recovery of the degradation system

Traditional chemical recovery of thermosetting polymers resorts to a high reaction temperature and a long reaction time, which causes uncontrollable degradation of the polymer. The decomposed products obtained under severe conditions were a complex mixture which was difficult to separate, and might produce secondary waste. Under our degradation conditions, the degradation product with a high M_w was insoluble in the reaction solution, so it was easy to separate by filtration, and the yield of the product could always reach nearly 100% (Fig. S8, ESI†). For the filtrate, it was easy to obtain the r-salt by concentration and crystallisation. The r-salt was $(NH_4)_2Ce(NO_3)_5{\cdot}4H_2O$ (Fig. 5) which can be used as an efficient catalyst for the synthesis of isoxazole derivatives, avoiding the oxidation and side reactions caused by cerium(IV).[37–39] The solvent could be reused in the degradation process. In particular, by tracking the whereabouts of the Ce and N elements in the system, about 98.89% of the cerium in the reactant was effectively recovered and more than 90% of the N element was found in the DSEP and r-salt, respectively (Fig. 6).

The degradation products contained hydroxyl, carbonyl, amino, and other polar groups, which had the potential for use in adhesives, and can be directly used without further processing. Different substrates, including aluminium, glass, FR-4 epoxy, and wood, were used to test the adhesion performance (Fig. 7). The degradation products showed good adhesion for most of the substrates except glass sheet. The bonding strength of the glass sheet was about 0.5 MPa whereas it was 1 MPa for the others, which was comparable to the formaldehyde-based adhesives. In addition, this was different from the thermosetting adhesives, and it could be easily recycled by solvent treatment. It was found that the adhesive showed good retention in repeated bonding experiments, indicating that the adhesion was thermally reconfigurable. The effect of temperature and time on the bonding strength was systematically examined further when applied to wood bonding (Fig. S9, ESI†). An adhesive strength of 0.66 MPa could be achieved by bonding at 40 °C whereas it was 0.89 MPa after bonding at 100 °C for 4 h. The degradation products are expected to be green and cost-efficient thermoplastic adhesives for plywood and could be used to replace formaldehyde-based adhesives. Compared with previous studies, the method was energy efficient and cost effective because it realises the full recovery and utilisation of the whole material and avoids additional extraction and neutralisation steps.

The recycling of CFRP

The CAN oxidation system was successfully extended to recycle the CFRP. The fibres could be better exposed after the resin was swollen, which was conducive to oxidative degradation. The recycled fibre was clean with no resin residue (Fig. 8). The recycled fibre retained 97.09% of the tensile strength of the original fibre even after reacting at 80 °C for 3 h (Fig. 9). The tensile strength was improved with the shortening of the reaction time, which indicated that the carbon fibre recovered had less tensile performance loss. For the resin degradation products ($DSEP_C$), it can form a uniform viscous liquid when mixed with acetone (Fig. S10a, ESI†), so the adhesive was obtained by this method and used for bonding of rigid

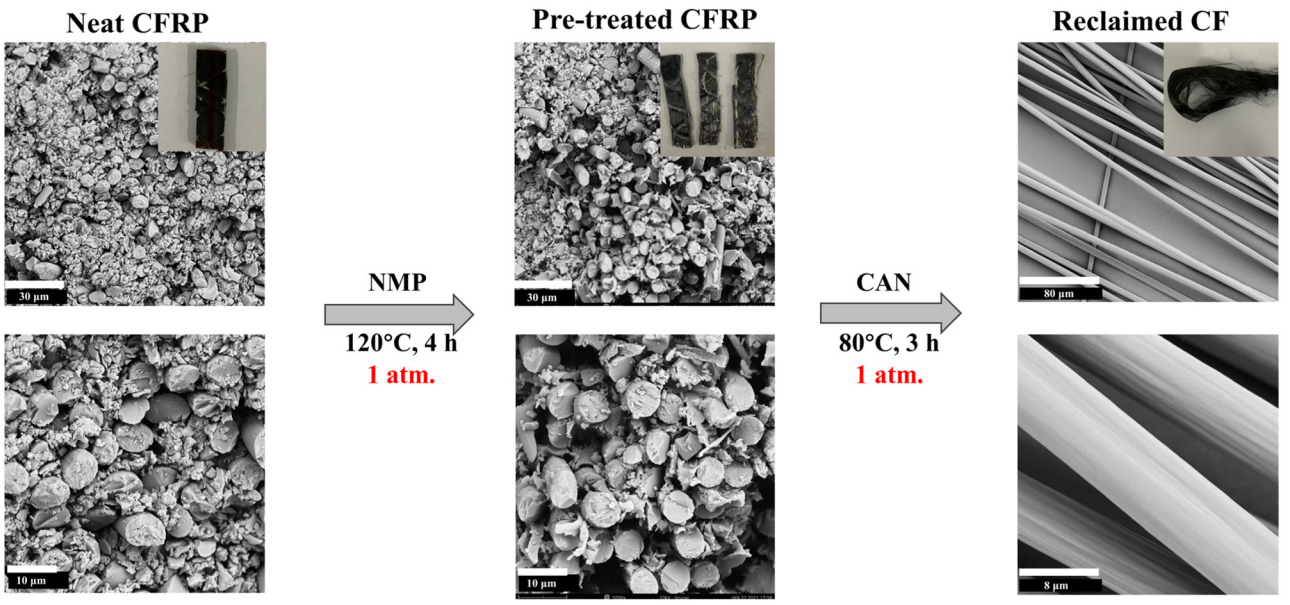

Fig. 8 Fast chemical recovery process of CFRP accelerated by microwave-assisted swelling using NMP.

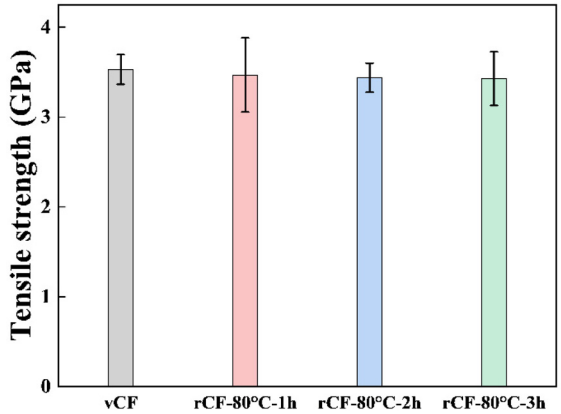

Fig. 9 Tensile strength of the virgin fibre and recycled fibre under different conditions.

material plates. Except for polytetrafluoroethylene (PTFE), the other plates could reach a bonding strength of 1.2 MPa.

Conclusions

In summary, an effective method is developed to completely degrade amine cured EP using CAN aqueous solutions and can achieve almost full recovery of all the materials. The recovery rate of resin degradation products is as high as 99%, whereas about 98.89% of the cerium and more than 90% of the N element were found in the system, respectively. Because of its special oxidation and acidity, the CAN could selectively cleave the hydroxyethyl ether unit and the C–N bond in EP, meanwhile, it retains the valuable main skeleton structure of EP. It is also found that the interaction between NMP and the hydroxyl groups in the resin hinders the further degradation, and thus leads to the high molecular weight of the degradation products. The revealed degradation mechanism provides a new method for adjusting the molecular weight of the degradation products. This oxidative system is successfully applied to the recovery of CFRP. The work provides a mild and feasible method for the chemical recovery of the amine cured epoxy resin.

Conflicts of interest

There are no conflicts to declare.

Acknowledgements

This work was supported by the National Natural Science Foundation of China (Grant No. 51721091) and the State Key Laboratory of Polymer Materials Engineering (Grant No. sklpme2020-1-02). Financial support is also provided by the Fundamental Research Funds for the Central Universities.

References

1 F.-L. Jin, X. Li and S.-J. Park, *J. Ind. Eng. Chem.*, 2015, **29**, 1–11.
2 K. Yang, S. Wu, J. Guan, Z. Shao and R. O. Ritchie, *Sci. Rep.*, 2017, **7**, 11939–11947.
3 J. Wan, J. Zhao, X. Zhang, H. Fan, J. Zhang, D. Hu, P. Jin and D.-Y. Wang, *Prog. Polym. Sci.*, 2020, **108**, 101287–101332.
4 S. Karuppannan Gopalraj and T. Kärki, *SN Appl. Sci.*, 2020, **2**, 433–453.
5 J. Zhang, V. S. Chevali, H. Wang and C.-H. Wang, *Composites, Part B*, 2020, **193**, 108053–108067.
6 S. Kumar and S. Krishnan, *Chem. Pap.*, 2020, **74**, 3785–3807.
7 C. A. Navarro, C. R. Giffin, B. Zhang, Z. Yu, S. R. Nutt and T. J. Williams, *Mater. Horiz.*, 2020, **7**, 2479–2486.
8 M. Shen, H. Cao and M. L. Robertson, *Annu. Rev. Chem. Biomol. Eng.*, 2020, **11**, 183–201.
9 J. M. Garcia and M. L. Robertson, *Science*, 2017, **358**, 870–872.
10 S. Wang, S. Ma, Q. Li, X. Xu, B. Wang, W. Yuan, S. Zhou, S. You and J. Zhu, *Green Chem.*, 2019, **21**, 1484–1497.
11 B. Wang, S. Ma, S. Yan and J. Zhu, *Green Chem.*, 2019, **21**, 5781–5796.
12 H. Yan, C. X. Lu, D. Q. Jing, C. B. Chang, N. X. Liu and X. L. Hou, *New Carbon Mater.*, 2016, **31**, 46–54.
13 I. Okajima, M. Hiramatsu, Y. Shimamura, T. Awaya and T. Sako, *J. Supercrit. Fluids*, 2014, **91**, 68–76.
14 M. Das and S. Varughese, *ACS Sustainable Chem. Eng.*, 2016, **4**, 2080–2087.
15 J. N. Lo, S. R. Nutt and T. J. Williams, *ACS Sustainable Chem. Eng.*, 2018, **6**, 7227–7231.
16 Y. J. Ma, C. A. Navarro, T. J. Williams and S. R. Nutt, *Polym. Degrad. Stab.*, 2020, **175**, 109125.
17 Y. J. Ma and S. Nutt, *Polym. Degrad. Stab.*, 2018, **153**, 307–317.
18 T. Hanaoka, Y. Arao, Y. Kayaki, S. Kuwata and M. Kubouchi, *ACS Sustainable Chem. Eng.*, 2021, **9**, 12520–12529.
19 D. H. Kim, M. Lee and M. Goh, *ACS Sustainable Chem. Eng.*, 2020, **8**, 2433–2440.
20 D. H. Kim, A. Yu and M. Goh, *J. Ind. Eng. Chem.*, 2021, **96**, 76–81.
21 T. Hanaoka, Y. Arao, Y. Kayaki, S. Kuwata and M. Kubouchi, *Polym. Degrad. Stab.*, 2021, **186**, 109537–109544.
22 F. Tian, X. L. Wang, Y. Yang, W. L. An, X. Zhao, S. M. Xu and Y. Z. Wang, *ACS Sustainable Chem. Eng.*, 2020, **8**, 2226–2235.
23 Y. J. Ma, D. Kim and S. R. Nutt, *Polym. Degrad. Stab.*, 2017, **146**, 240–249.
24 W. R. Dang, M. Kubouchi, H. Sembokuya and K. Tsuda, *Polymer*, 2005, **46**, 1905–1912.
25 M. Das, R. Chacko and S. Varughese, *ACS Sustainable Chem. Eng.*, 2018, **6**, 1564–1571.

26 K. Zheng, Q. Zou, Y. Yang, Y. Mao, J. Zhang and J. Cheng, *Ind. Eng. Chem. Res.*, 2018, **57**, 13283–13290.
27 T. Deng, Y. Liu, X. Cui, Y. Yang, S. Jia, Y. Wang, C. Lu, D. Li, R. Cai and X. Hou, *Green Chem.*, 2015, **17**, 2141–2145.
28 Y. Wang, X. Cui, H. Ge, Y. Yang, Y. Wang, C. Zhang, J. Li, T. Deng, Z. Qin and X. Hou, *ACS Sustainable Chem. Eng.*, 2015, **3**, 3332–3337.
29 W.-B. Pan, L.-M. Wei, L.-L. Wei, C.-C. Wu, F.-R. Chang and Y.-C. Wu, *J. Chem. Res., Synop.*, 2005, **52**, 581–588.
30 G. G. a. B. Rindone, *Chem. Soc. Rev.*, 1979, **9**, 828–832.
31 X. Yang, C. Xi and Y. Jiang, *Tetrahedron Lett.*, 2005, **46**, 8781–8783.
32 H. Fujioka, Y. Ohba, H. Hirose, K. Murai and Y. Kita, *Org. Lett.*, 2005, **7**, 3303–3306.
33 V. Nair and A. Deepthi, *Chem. Rev.*, 2007, **107**, 1862–1891.
34 Z. Q. Zhang, T. Chen and F. M. Zhang, *Org. Lett.*, 2017, **19**, 1124–1127.
35 H. Firouzabadi, N. Iranpoor and A. Khoshnood, *J. Mol. Catal. A: Chem.*, 2007, **274**, 109–115.
36 H. Firouzabadi, N. Iranpoor and F. Nowrouzi, *Chem. Commun.*, 2005, **41**, 789–791.
37 N. Audebrand, J. P. Auffredic and D. Louer, *Thermochim. Acta*, 1997, **293**, 65–76.
38 K. Tanemura, T. Suzuki, Y. Nishida, K. Satsumabayashi and T. Horaguchi, *J. Chem. Res., Synop.*, 2003, **8**, 497–499.
39 K.-i. Itoh and C. A. Horiuchi, *Tetrahedron*, 2004, **60**, 1671–1681.